Petroleum Science 21 (2024) 3621–3629

Contents lists available at ScienceDirect

Petroleum Science

journal homepage: www.keaipublishing.com/en/journals/petroleum-science

Original Paper

Inhibition of wax crystallization and asphaltene agglomeration by core-shell polymer@SiO_2 hybride nano-particles

Xin-Yuan Li [a], Xu-Biao Zhang [a], Si-Bei Li [a], Li-Wei Hui [a], Xin-Jie Sun [b], Jun Xu [b, c, *]

[a] Sino Oil King Shine Chemical Co., Ltd., Langfang, 065000, Hebei, China
[b] School of Chemical Engineering, East China University of Science and Technology, Shanghai, 200237, China
[c] Large Industrial Reactor Engineering Research Center of Ministry of Education, East China University of Science and Technology, Shanghai, 200237, China

ARTICLE INFO

Article history:
Received 12 October 2023
Received in revised form
4 June 2024
Accepted 4 June 2024
Available online 5 June 2024

Edited by Min Li

Keywords:
Heavy oil
Wax crystallization
Asphaltene agglomeration
Hybride nanoparticle
Viscosity reduction

ABSTRACT

The gelation of crude oil with high wax and asphaltene content at low temperatures often results in the block of transportation pipeline in Africa. In recent years, it was reported that surface hydrophobic-modified nanoparticles have important applications in crude oil flow modification. In this work, four kinds of core-shell hybride nanoparticles by grafting poly (octadecyl, docosyl acrylate) and poly (acrylate-α-olefin) onto the surface of nano-sized SiO_2 were synthesized by grafting polymerization method. The chemical structure of nanoparticles was analyzed by Fourier transform infrared spectroscopy (FT-IR), scanning electron microscopy (SEM) and thermogravimetric analysis (TGA). The rheological behaviors of crude oil and precipitation of asphaltenes in the presence of nanoparticles were studied by measuring the viscose-temperature relationship curve, the cumulative wax precipitation amount, and morphology of waxes and asphaltenes. The results indicate that the docosyl polyacrylate@SiO_2 nanoparticle (PDA@SiO_2) can reduce the cumulative wax precipitation amount of crude oil by 72.8%, decline the viscosity of crude oil by 85.6% at 20 °C, reduce the average size of wax crystals by 89.7%, and inhibit the agglomeration of asphaltene by 74.8%. Therefore, the nanoparticles not only adjust the crystalline behaviors of waxes, but also inhibit the agglomeration of asphaltenes. Apparently, core-shell hybride nanoparticles provides more heterogeneous nucleation sites for the crystallization of wax molecules, thus inhibiting the formation of three-dimensional network structure. The core-shell polymer@SiO_2 hybride nanoparticles are one of promising additives for inhibiting crystallization of waxes and agglomeration of asphaltenes in crude oil.

1. Introduction

With the rapid development of the world economy, the demand for energy is gradually increasing nowadays. As the reserves of light oil are sharply declined due to excessive exploitation and consumption, the extraction and utilization of heavy crude oil, has attracted more and further attention (Adeyanju and Oyekunle, 2019; Alimohammadi et al., 2019; Li et al., 2019). However, with the continuous extraction of heavy crude oil, such as African crude oil, the external conditions (e.g., temperature and pressure) or the composition of the heavy crude oil has been changed, thus wax content and asphaltene content of oil have gradually increased. Generally, the fluidity of crude oil is closely related to its internal waxes and asphaltenes content, structure and growth process. With the decrease of external temperature, the solubility of wax components in crude oil decreases sharply, which leads to its precipitation. When the waxes and asphaltenes aggregate and precipitate out of the crude oil, which often block the transportation pipeline, and bring huge obstacles to the safe and economic operation of oil transportation (Adeyanju and Oyekunle, 2019; Hasan et al., 2010). To solve the aforesaid problem, many physical approaches (such as heating and oil blending) and chemical approaches (such as emulsification, microbial method, and oilfield reagent injection) have been applied. In the above methods, injecting oilfield reagent has a lot of advantages, such as low energy consumption, less processing cost, fewer environmental pollution, and prosperous market potential. Therefore, it is requisite to develop a new and efficient chemical additive to solve the problem of pipeline blockage today.

* Corresponding author. School of Chemical Engineering, East China University of Science and Technology, Shanghai, 200237, China.
E-mail address: xujun@ecust.edu.cn (J. Xu).

https://doi.org/10.1016/j.petsci.2024.06.003

Up to now, new materials derived from nanotechnology have been used in the petroleum industry (Corredor et al., 2019; Gaihre et al., 2018; Kumar et al., 2012; Li et al., 2018). Compared to traditional pour-point depressants (PPDs), nano-composite materials have high surface effects, and are easily dispersed into crude oil and adsorbed on the surface of waxes, colloids, and asphaltenes (Deshmukh and Bharambe, 2008; Huang et al., 2018; Jia et al., 2008; Jing et al., 2017). Among the numerous of nanomaterials, nano-SiO_2 is wildly applied because of its large specific surface area, good chemical and thermal stability. In addition, abundant hydroxyl groups on the surface of nano-SiO_2 can be substituted by other groups, which bring high surface activity and designability to themselves (Oyekunle and Adeyanju, 2011; Taborda et al., 2017). Therefore, composites of conventional PPDs and SiO_2 nanoparticles are applied to enhance the performance (Mohammadi et al., 2011; Yan et al., 2017). Poly (octadecyl acrylate)/clay nano-composite prepared by melt blending can reduce the viscosity of gelled waxy crude oil (Mao et al., 2020; Yao et al., 2016a). Serving as wax nucleation centers, this nanocomposite effectively inhibits the formation of viscoelastic gel network. Compared with poly (octadecyl acrylate), nano-composites impair the structural strength and reduce the viscoelasticity of gelled crude oil. Therefore, they can improve the rheological properties of waxy crude oils (Ning et al., 2022; Norrman et al., 2016; Yao et al., 2016a, 2016b). In other studies, in the presence of nano-SiO_2 composites synthesized by surface-modification and copolymerized with styrene, butyl methacrylate and acrylamide (molar ratio of 9:10:0.8) (Qing et al., 2020), the viscosity of waxy crude oil was reduced by 90.1%. Since nano-composites can also be adsorbed on the surface of asphaltenes for their high surface area and activity, they have the capability of inhibiting the agglomeration of asphaltenes. But such studies are rarely reported. Belal and Maen (2012) found that NiO nanoparticles prepared in situ within heavy oil display much higher affinity toward asphaltenes adsorption. Further experiments have shown that the adsorption effect of the NiO nanoparticles on asphaltene has exceeded that of commercial NiO nanoparticles of the same size range. Kazemzadeh et al. (2015) found that, in solutions without nanoparticles, a high *n*-heptane content improves the asphaltene adsorption onto the nanoparticles which implies less asphaltene flocculation and precipitation.

In this work, a series of core-shell nano-composites by grafting poly (octadecyl, docosyl acrylate) and poly (acrylate-α-olefin) onto the surface of nano-sized SiO_2 were synthesized by surface-grafting polymerization method. The structure of as-prepared nano-composites were characterized by FT-IR, SEM and TGA. The rheological property and wax crystallization behaviors of African crude oil were investigated by differential scanning calorimeter (DSC), viscosity, yield stress and thixotropy. In addition, the effect of nanoparticles on the asphaltene agglomeration behaviors was investigated by the initial precipitation point test and microscope of asphaltenes. The results show that nanoparticles not only suppress the crystallization of waxes, but also inhibit the agglomeration of asphaltenes in crude oil.

2. Experimental

2.1. Materials

γ-Methacryloxypropyltrimethoxysilane (KH570, 99%), anhydrous ethanol (≥99.0%), methanol (99%), *n*-heptane, toluene (≥99.0%), xylene (99%), octadecyl methacrylate (SA, 99%), α-20~24 olefin and α-24~28 olefin were purchased from Shanghai Aladdin Biochemical Technology Co., Ltd. The abenzoyl peroxide (BPO, 99%) was purchased from Tianjin Zhiyuan Chemical Reagent Co., Ltd. And nano silica (SiO_2, 20 nm) was purchased from Xiya Chemical Technology (Shandong) Co., Ltd. The docosyl acrylate (DA) was synthesized by ourselves in the laboratory (Li et al., 2021). The crude oil is obtained from Africa oil field, and its properties are shown in Table 1.

2.2. Grafting polyacrylate onto the surface of nano-sized SiO_2

For instance, 1.0 g silane coupling agent KH570 and 200.0 g ethanol-water solution (the volume ratio of ethanol to water is 9:1) was added into a three-necked flask, stirred at 30 °C for 1.5 h. Then 10.0 g nano-SiO_2 was added into the above solution, and the reaction was conducted at 75 °C with reflux condensation for 3 h. After reaction, the obtained KH570@SiO_2 product was centrifuged out and dried overnight at 60 °C.

Synthesis of polyacrylate@SiO_2 nano-composite (PSA, PDA@-SiO_2). 10.0 g octadecyl methacrylate (SA) and 10.0 g KH570@SiO_2 were added into the flask with toluene as a solvent, which were completely dissolved at 60 °C with the help of ultrasound. Then, 0.5 g benzoyl peroxide (BPO) was added in and the temperature was raised to 90 °C. After reaction for 8 h under the protection of N_2, the obtained crude product was centrifuged out and washed with toluene. This process was repeated for 3 times to remove unreacted monomers and impurities. After drying, the octadecyl polyacrylate@SiO_2 nanoparticle (PSA@SiO_2) was acquired. Similarly, the docosyl polyacrylate@SiO_2 nanoparticle (PDA@SiO_2) was synthesized by the same method.

Synthesis of poly (acrylate-α-olefin)@SiO_2 nano-composite (PSA-20~24, PSA-24~28@SiO_2). 50.0 g octadecyl acrylate monomer, 9.5 g α-20~24 olefin and 10.0 g KH570@SiO_2 were added into the flask with *o*-xylene as solvent. Then 2.0 g benzoyl peroxide was added into the flask as an initiator. Under the protection of nitrogen, the polymerization reaction maintained at 90 °C for 8 h. The crude product was purified by distilling the solvent, washed with toluene and centrifuged for 3 times. Finally, poly (acrylate-α-20~24 olefin)@SiO_2 (PSA-20~24@SiO_2) was acquired. Similarly, poly (acrylate-α-24~28 olefin)@SiO_2 (PSA-24~28@SiO_2) was synthesized by the same method.

2.3. Characterization

The functional groups of the nano-composite structure were characterized and analyzed by FT-IR spectroscopy (IR Prestige-21, Shimadzu). The grafting rate of polyacrylate onto the surface of nano-sized SiO_2 was measured by using TGA (STA449F3, Netzsch). In TGA tests, the temperature range is 25–800 °C and the heating rate is 10 °C/min. The morphology of nano-composites were observed by SEM (S-3400, Hitachli).

Table 1
Fundamental properties of African crude oil.

Property	Value
Density, g/cm^3	0.8669
Water content, %	0.35
WAT, °C	53.86
Sulfur content, %	0.0922
Pour point, °C	33
Moisture content, %	0.3514
Saturates hydrocarbon, %	36.35
Aromatic hydrocarbon, %	19.73
Asphaltene, %	11.97
Resin, %	31.95

2.4. Rheological measurements

The oil samples were prepared by adding 1000 mg/kg different nanoparticles into the crude oil. Before testing, all of the oil samples were heated at 80 °C for 30 min.

In the presence of synthetic nano-composites, the viscosity, yield stress and thixotropy of crude oil were measured by using an Anton Paar rotary rheometer (MCR501, Austria). The viscosity of oil sample was measured from 80 to 10 °C in 1 °C/min at a shear rate of 10 s^{-1}. During the yield stress measurements, oil samples were heated to 80 °C and cooled down to 50 °C with 10 °C/min. When the temperature was invariant, the yield stress tests were performed with shear stress increasing logarithmically in the range of 0.01–1000 Pa. The thixotropic tests were performed with shear rate increasing from 0 to 10 s^{-1} and decreasing from 10 to 0 s^{-1}.

2.5. Was crystallization behaviors

Wax appearance temperature (WAT) and wax precipitation curve of crude oil were investigated by differential scanning calorimeter (DSC-Q2000, TA). The amount of wax precipitation at the test temperature was calculated by integral method. The test temperature range is 80–10 °C, and the cooling rate is 5 °C/min.

The crystal configuration of wax was investigated by using a polarizing microscope (DM2500P, Leica). The images were captured and analyzed by the software Image J.

2.6. Inhibition of asphaltene aggregation tests

By adding varying volume fractions of *n*-heptane to crude oil, the sudden increase of viscosity for crude oil at different temperature is defined the initial precipitation point (IPP) of asphaltene (Yang et al., 2015). The viscosity curves with different content of *n*-heptane at different temperature were measured by using an Anton Paar rotary rheometer (MCR501, Austria). In addition, the morphology of asphaltene aggregates were investigated using an optical microscope (DM2500P, Leica) (see Fig. 1).

3. Results and discussion

3.1. Chemical structure characterization of nano-composites

In order to verify whether copolymers are successfully grafted with nano-SiO_2, the characteristic functional groups of nano-composites are analyzed by FT-IR spectroscopy (Fig. 2). As shown in Fig. 2(a), in the infrared spectrum of SiO_2, absorption at 3450 cm^{-1} is from the stretching vibration of −OH bond. Absorption at 1630 cm^{-1} is due to bending vibration of H−O−H bond, and that at 1112 cm^{-1} is from asymmetric vibrations of Si−O−Si groups. Comparatively, for modified SiO_2, adsorption at 2925 and 2850 cm^{-1} are from the stretching vibration absorption of $-CH_2-$ bond (Table S1). The intensity of absorption at 3450 cm^{-1} from Si−OH bond is weakened, which indicates that the number of hydroxyl groups on the surface of SiO_2 decreases. The reduction of hydroxyl groups proves that KH570 is successfully grafted on the surface of nano-SiO_2. In the spectra of polyacrylate@SiO_2 (Fig. 2(b)), the presence of absorptions at 1050–1300 cm^{-1} is from C=O and C−O−C bonds, which indicates the existence of ester group. In addition, from Table S1, adsorptions at 2925, 2850 and 1470 cm^{-1} are due to the stretching vibration of $-CH_2-$ group. Absorption at 720 cm^{-1} attributed to a $-(CH_2)_n-$ bridge ($n \geq 4$) group are also present. It shows that the nanoparticles by grafting polyacrylate onto the surface of nano-sized SiO_2 were successfully synthesized.

The grafting rate of polyacrylate onto the surface of nano-sized SiO_2 is analyzed by TGA (Fig. 3). In the temperature range of 200–800 °C, the grafted polymer is gradually decomposed, ultimately only SiO_2 is remained. Therefore, the calculation formula for grafting rate is $(W_0-W_1)/W_0$, where W_0 represents the quality of nano-composite before testing, and W_1 represents the quality of nano-silica after testing. As shown in Fig. 3, the grafting rate of PSA@SiO_2, PDA@SiO_2, PSA-20~24@SiO_2 and PSA-24~28@SiO_2 are 49.5%, 54.1%, 46.1% and 47.7%, respectively.

The morphology of nano-SiO_2 before and after grafting polymers are observed by SEM (Fig. S1). Since the high polarity of hydroxyl groups on the surface of SiO_2, the agglomeration of particles is apparent. However, for the KH570 grafted SiO_2, it is found that the dispersion of particles is improved. In addition, after the grafting of PDA, the size of particles slightly increases, but the interface between particles is clear, which indicates that the dispersion of particles is significantly improved.

3.2. Wax crystallization behaviors of crude oil in the presence of nano-composites

In the presence of different nano-composites, the DSC curves of crude oil are investigated (Fig. 4). From Fig. 4(a), the initial wax appearance temperature (WAT) and crystallization enthalpy of crude oil are 53.86 °C and 0.95 J/g, respectively. The second wax

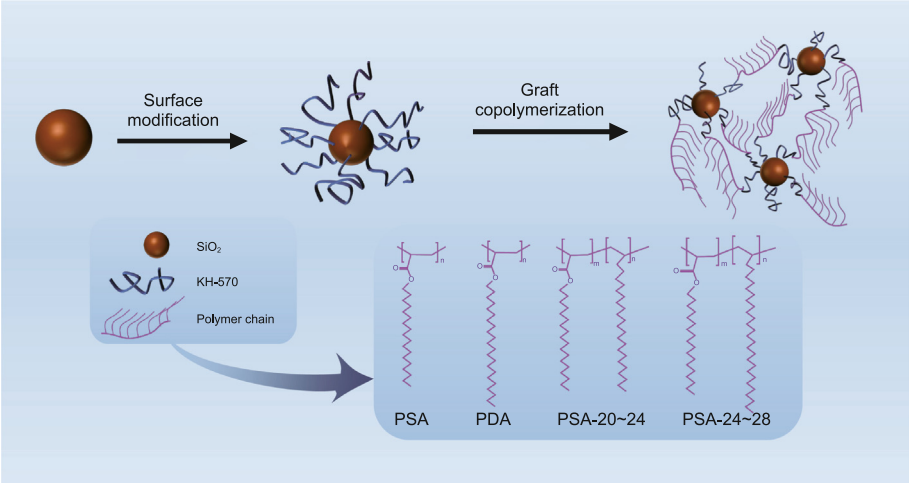

Fig. 1. Schematic diagram of the synthesis of polymer@SiO_2 nano-composites.

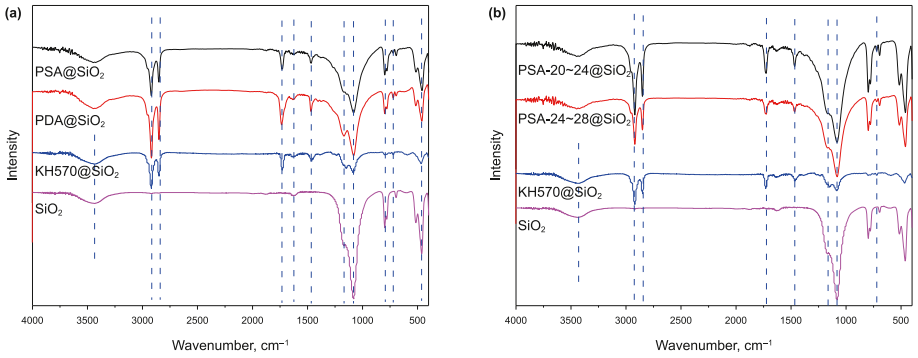

Fig. 2. FT-IR spectroscopy of **(a)** SiO_2, KH570@SiO_2, PSA@SiO_2 and PDA@SiO_2; **(b)** SiO_2, KH570@SiO_2, PSA-20~24@SiO_2 and PSA-24~28@SiO_2

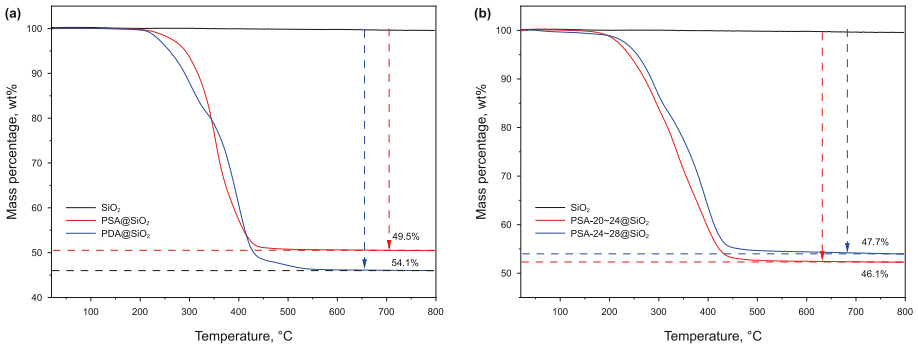

Fig. 3. TGA curves of **(a)** SiO_2, PSA@SiO_2 and PDA@SiO_2; **(b)** SiO_2, PSA-20~24@SiO_2 and PSA-24~28@SiO_2.

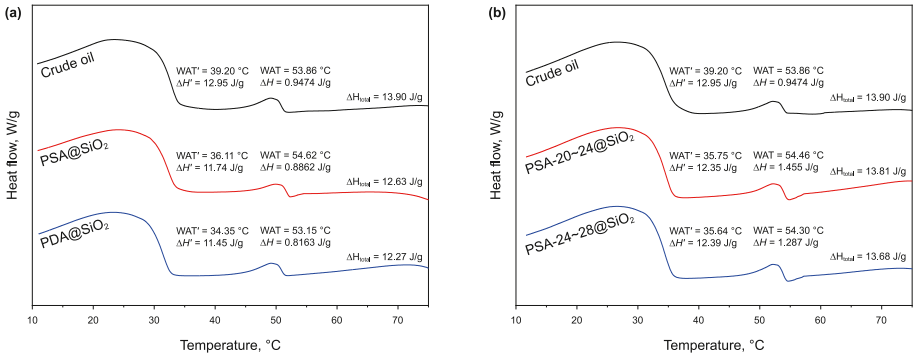

Fig. 4. DSC curves of crude oil with adding different nano-composites, **(a)** crude oil, PSA@SiO_2 and PDA@SiO_2; **(b)** crude oil, PSA-20~24@SiO_2 and PSA-24~28@SiO_2

appearance point (WAT') and crystallization enthalpy corresponding to low-carbon wax are 39.20 °C and 12.95 J/g, respectively. After adding PSA@SiO_2 and PDA@SiO_2, the WAT and corresponding crystallization enthalpy show no obvious change. But the WAT' of crude oil decreases from 39.20 °C to 36.11 and 34.35 °C, and crystallization enthalpy of low-carbon wax decreases from 12.95 J/g to 11.74 and 11.45 J/g, respectively. The total crystallization enthalpy of crude oil decreases from 13.90 J/g to 12.63 and 12.27 J/g, respectively.

Similarly, from Fig. 4(b), after adding PSA-20~24@SiO_2 and PSA-24~28@SiO_2, all the WAT' of crude oil decreases from 39.20 °C to 35.75 and 35.64 °C, and crystallization enthalpy for low-carbon wax decreases from 12.95 J/g to 12.35 and 12.39 J/g, respectively. And the total crystallization enthalpy of crude oil decreases from 13.90 J/g to 13.81 and 13.68 J/g, respectively. Consequently, the total crystallization enthalpy reduced by the composite particles follows the sequence of PDA@SiO_2 > PSA@SiO_2 > PSA-24~28@SiO_2 > PSA-20~24@SiO_2.

High freezing point and yield value of waxy crude oil is generally caused by paraffin precipitation at low temperatures and formation of a three-dimensional network structure (Liu et al., 2021; Mahmoud and Betiha, 2021). Apparently, in the presence of nano-composites (PSA@SiO_2, PDA@SiO_2, PSA-20~24@SiO_2, PSA-24~28@SiO_2), the wax precipitation amount of crude oil decreased from 13.64 wt% to 11.79, 10.52, 11.53, 11.45 wt%, respectively (Fig. 5). The wax precipitation amount reduced by composite particles follows the sequence of PDA@SiO_2 > PSA-24~28@SiO_2 > PSA-20~24@SiO_2 > PSA@ SiO_2. Therefore, in the temperature range 10–40 °C, all of four composite particles can inhibit the precipitation of wax crystals in crude oil, in which PDA@SiO_2 shows the best effect.

The influence of KH570@SiO_2, PDA and PDA@SiO_2 on wax

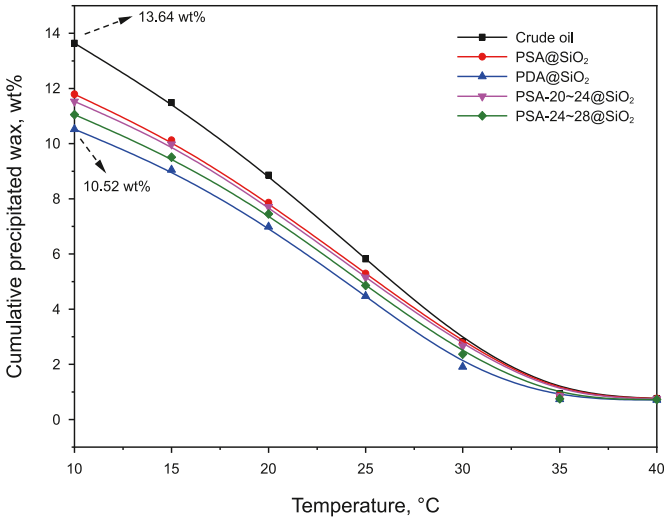

Fig. 5. The quantity of wax precipitated from crude oil without and with different nano-composites.

crystallization behaviors of crude oil are investigated (Fig. 6). After adding KH570@SiO_2 and PDA, the WAT of crude oil increase from 53.86 °C to 57.56 and 54.48 °C, but the WAT' decrease from 39.20 °C to 36.05 and 35.78 °C. Total crystallization enthalpy of crude oil decreases from 13.90 J/g to 14.24 and 13.55 J/g, respectively. With the addition of PDA@SiO_2, the WAT of crude oil shows no obvious change, but the WAT' decreases from 39.20 to 34.35 °C. And the total crystallization enthalpy of crude oil decreases from 13.90 to 12.27 J/g. In summary, compared to KH570@SiO_2 and PDA, PDA@-SiO_2 can better reduce the WAT' and the total crystallization enthalpy of crude oil.

3.3. Flowability at low temperature of crude oil in the presence of nano-composites

In the presence of different nano-composites, the viscosity-temperature behaviors of crude oil are investigated by rheological method (Fig. 7). From this figure, in the presence of PSA@SiO_2 and PDA@SiO_2, the viscosity of crude oil is apparently declined. The viscosity reduction of crude oil at 20 °C by PSA@SiO_2 and PDA@SiO_2 are 57.2% and 85.6%, respectively. At the same temperature, the viscosity is reduced by 60.4% in the presence of PSA-24~28@SiO_2, while only 29.1% in the presence of PSA-20~24@SiO_2. The viscosity reduced by the nano-composites following the sequence of PDA@SiO_2 > PSA-24~28@SiO_2 > PSA@SiO_2 > PSA-20~24@SiO_2. Therefore, at lower temperature ranges, the viscosity is reduced most by PDA@SiO_2, which is also consistent with the results of wax crystallization behaviors revealed by DSC.

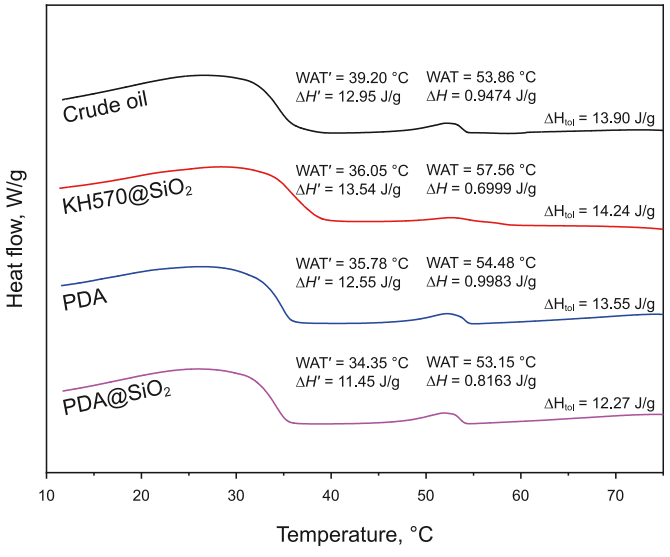

Fig. 6. DSC curves of crude oil in the presence of KH570@SiO_2, PDA and PDA@SiO_2

The effect of PDA@SiO_2 concentration (500, 1000, 1500 and 2000 ppm) on the rheological behaviors of crude oil are also investigated (Fig. S2). The reduction of crude oil viscosity with different nano-composite concentration at 20 °C is shown in Table S2. When the concentration is 500 ppm, the reduction of viscosity reaches 66.7%, from 40087 to 13348 mPa s. When the dosage increases to 1000 ppm, the viscosity of crude oil is reduced most and the reduction rate is 85.6%. However, when the concentration is increased to 1500 and 2000 ppm, the reduction rate of viscosity is decreased from 85.6% to 71.1% and 70.1%, respectively. It indicates that nano-composites with a high concentration are unfavorable for improving the flowability at low temperature of crude oil.

In the presence of PDA@SiO_2, the thixotropic property and yield stress of crude oil are investigated (Fig. 8). The thixotropic property reflects the recovery ability and structural strength of crude oil gel structure. In Fig. 8(a), the hysteresis ring area of crude oil decreases obviously after adding PDA@SiO_2 and the reduction rate is 60.1%. In addition, the shear stress of crude oil also decreases, which indicates that the flowability of crude oil is improved. From Fig. 8(b), in the presence of PDA@SiO_2, the yield stress value of crude oil decreases from 240 to 90 Pa and the reduction rate is 62.5%, which indicates that the structural strength of gel in crude oil is impaired.

3.4. Wax crystal morphology analysis

The morphology of wax crystals in the presence of KH570@SiO_2, PDA and PDA@SiO_2 into crude oil are investigated (Fig. 9). As shown in Fig. 9(a), the wax crystals exhibit a long needle-like structure and the average statistical size is 340 μm (Table 2). In the presence of KH570@SiO_2 (Fig. 9(b)), although the wax crystals mainly needle-like structure, but the size is much shorter, which is reduced to 325 μm. In the presence of PDA and PDA@SiO_2 (Fig. 9(c)–(d)), the wax crystals exhibit short needle and irregular complex structures, and the average sizes of wax crystals are reduced to 77 and 35 μm, respectively.

Fig. 10(a)–(b) show the statistical size analysis and statistical area analysis of wax crystals precipitated in crude oil, respectively. As shown in Fig. 10(a), after adding PDA@SiO_2 nanoparticles to crude oil, the size of the precipitated wax crystals is the smallest. In addition, the area in Fig. 10(b) indicates the amount of wax crystals precipitated in the crude oil. After adding PDA@SiO_2 nanoparticles, the wax crystals precipitated the least in crude oil, and the precipitation amount decreased from 21.17% to 12.28%. Compared to other nanoparticles, PDA@SiO_2 exhibits the best inhibitory effect on the precipitation of wax crystals in crude oil, which is consistent with previous experimental conclusions. In general, hydrophobic nano-composite particles can provide plenty of heterogeneous nucleation sites for wax crystallization, resulting in a much smaller size of wax crystals (Soni and Bharambe, 2008; Soni et al., 2010). Therefore, as the wax crystal size continues to decrease, the flowability of crude oil is gradually improved, which is also consistent with DSC and rheological results.

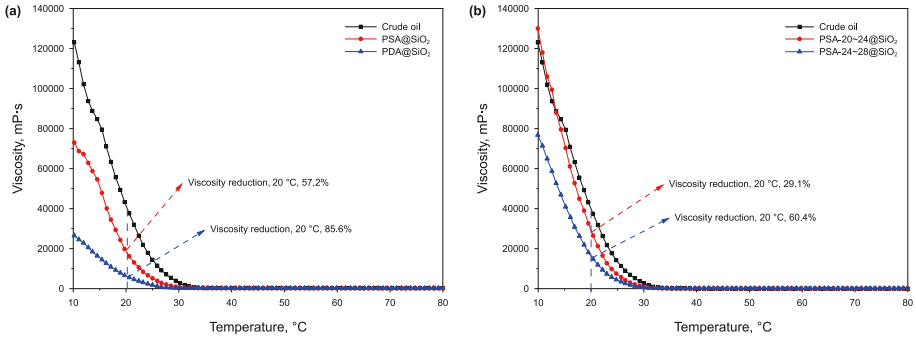

Fig. 7. Effect of different nano-composites on the viscosity-temperature behaviors of **(a)** crude oil, PSA@SiO_2 and PDA@SiO_2; **(b)** crude oil, PSA-20~24@SiO_2 and PSA-24~28@SiO_2.

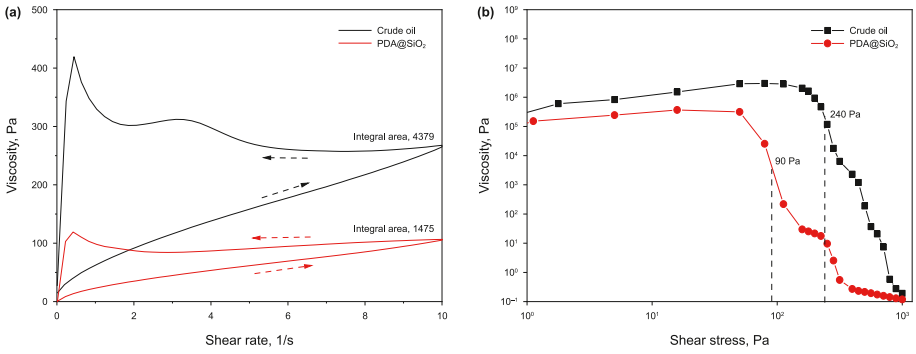

Fig. 8. **(a)** Thixotropy curve and **(b)** yield stress curve of crude oil in the presence of PDA@SiO_2

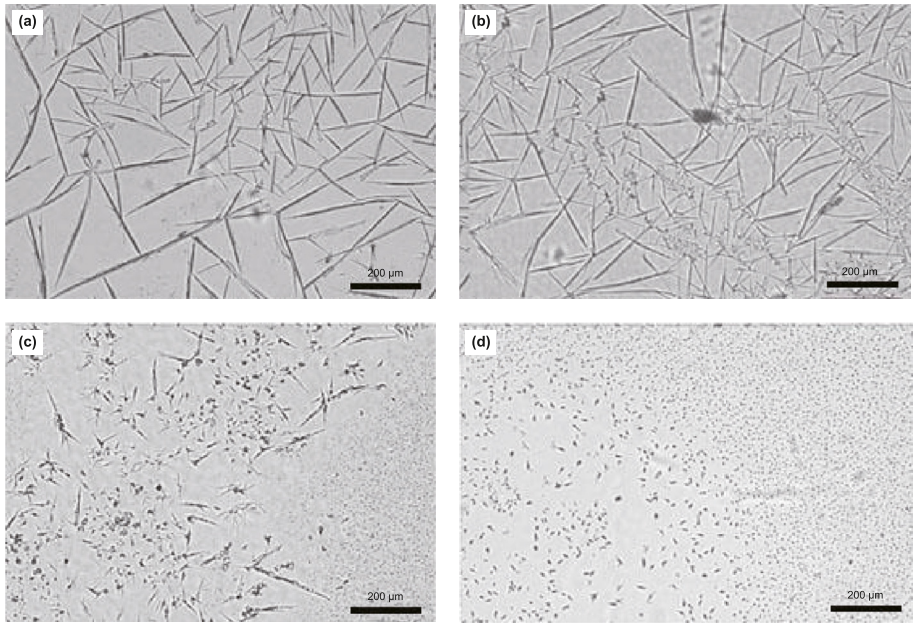

Fig. 9. Microscopic images of wax crystals in crude oil with and without nano-composites, **(a)** crude oil; **(b)** KH570@SiO_2; **(c)** PDA; **(d)** PDA@SiO_2.

3.5. Inhibition of asphaltene agglomeration

As we all know, asphaltene is soluble in toluene, but insoluble in *n*-heptane. Therefore, if adding different volume fractions of *n*-heptane to crude oil, the flocculation and deposition of asphaltenes will be changed. To investigate it, the viscosity-temperature behaviors of crude oil are tested (Fig. S3). It can be seen that, when the temperature is above 30 °C, the viscosity of crude oil is still very low after adding *n*-heptane, indicating that no obvious precipitation of asphaltenes is happened. Besides, the viscosity changes of crude oil at low temperature (15, 20, 25, 30 °C) are investigated (Fig. 11(a)). Apparently, after the dosage of *n*-heptane, the viscosity of crude oil gradually decreases. Nevertheless, when the volume content of *n*-heptane reaches 23%, the viscosity of the oil sample abruptly begins

Table 2
Average statistical size of wax crystal of crude oil with and without nanocomposites.

Category	Average statistical size of wax crystal, μm
crude oil	340
KH570@SiO_2	325
PDA	77
PDA@SiO_2	35

to increase, which is defined as the initial precipitation point (IPP). When the content is beyond IPP, the viscosity of crude oil drops, which generates a bulge. The appearance of bulge indicates that asphaltene have experienced agglomeration and deposition. Moreover, with the decrease of temperature, the bulge becomes more obvious, which indicates that the deposition of asphaltenes increases accordingly.

The influence of PDA@SiO_2 on the deposition of asphaltenes in crude oil was also investigated (Fig. 11(b)). After adding PDA@SiO_2 into the crude oil, the IPP is increased and the viscosity at the bulge is largely reduced. Compared with the crude oil without any additive, the bulge area is reduced by 74.8%, which further shows that PDA@SiO_2 can effectively inhibit asphaltene agglomeration and deposition.

In the presence of *n*-heptane and PDA@SiO_2, the morphology of asphaltene aggregates is investigated (Fig. 12). From Fig. 12(a), a small amount of asphaltene aggregates are suspended in crude oil, and no obvious large aggregates is found. However, after adding 25% *n*-heptane, a large number of aggregates are found in the oil phase (Fig. 12(b)). When both *n*-heptane and PDA@SiO_2 are added into the crude oil (Fig. 12(c)), the size of asphaltenes decreases obviously, which indicates that PDA@SiO_2 can well inhibits the agglomeration of asphaltenes. By statistically analyzing the average particle size of asphaltene aggregates (Fig. 12(d)–(f)), they are 3.75, 6.52 and 4.35 μm, which further confirms the microscopic observation.

3.6. Possible mechanism

In order to understand the flowability of crude oil after adding core-shell composite nanoparticles, a possible mechanism is proposed (Fig. 13). Due to their large specific surface area and polar surface, nanoparticles are particularly prone to agglomeration in the oil phase. The agglomerated particles cannot provide sufficient nucleation sites for wax crystallization. Therefore, they cannot reduce the size of wax crystals and improve the flowability at low temperature of crude oil.

After grafting the suitable polymers, core-shell composite nanoparticles, as heterogeneous nucleation sites, largely change the crystallization behaviors of waxes, which hinder the formation of three-dimensional network structure. Moreover, the long aliphatic chains of polyacrylate can attract asphaltenes through the hydrophobic association and adsorb on the surface of asphaltenes. Meanwhile, these long aliphatic branches also generate steric hindrance (repulsion) between surrounding asphaltenes, thereby avoiding the formation of stable and large-sized agglomeration of asphaltenes. When the aliphatic branches are short, the attraction outweighs the repulsion. But when they are longer, it is vice versa. The attraction is fundamental to the action of the composite particles. If they cannot be adsorbed on the asphaltene surface, the composite particles cannot play a role. But if there is only attraction, but no repulsion, asphaltenes cannot be dispersed. So, there must be a point where the two balance out. It also explains why there is a reasonable aliphatic length.

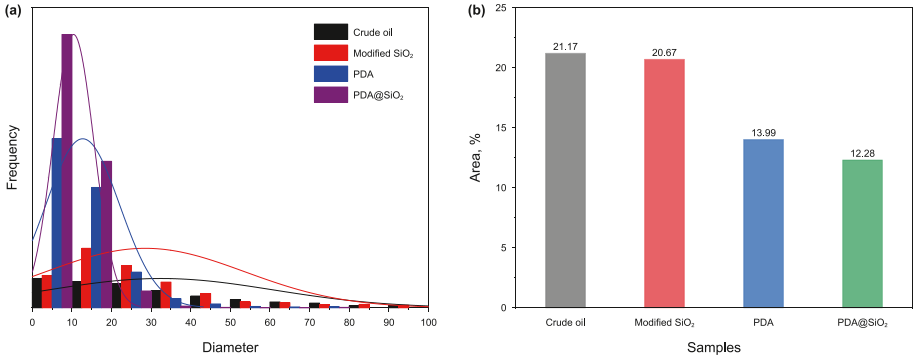

Fig. 10. **(a)** Statistical size analysis and **(b)** statistical area analysis of wax crystals precipitated from crude oil.

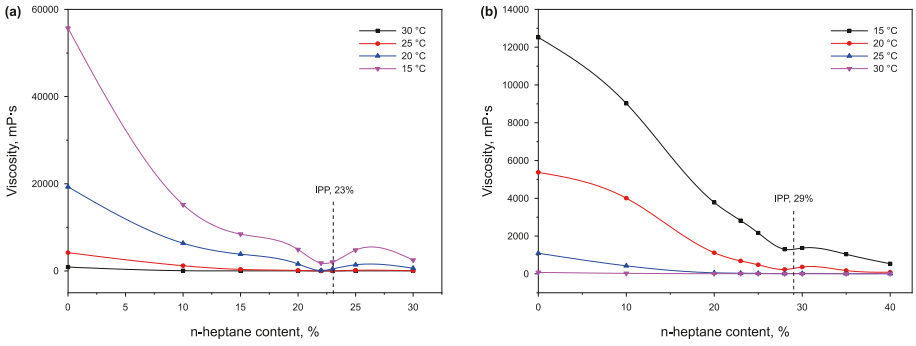

Fig. 11. Viscosity of crude oil **(a)** before and **(b)** after adding PDA@SiO_2 with different volume content of *n*-heptane at different temperature.

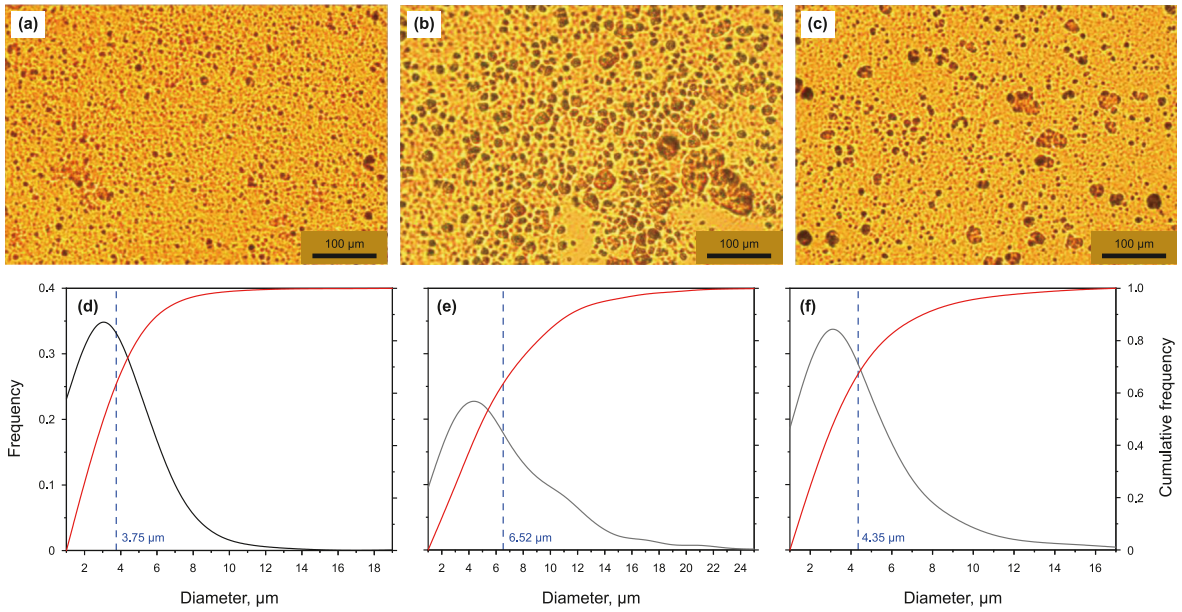

Fig. 12. Microscopic images and average particle size distribution of asphaltenes in crude oil with **(a)**, **(d)** no additive; **(b)**, **(e)** 25% *n*-heptane; **(c)**, **(f)** 25% *n*-heptane + 1000 ppm PDA@SiO_2.

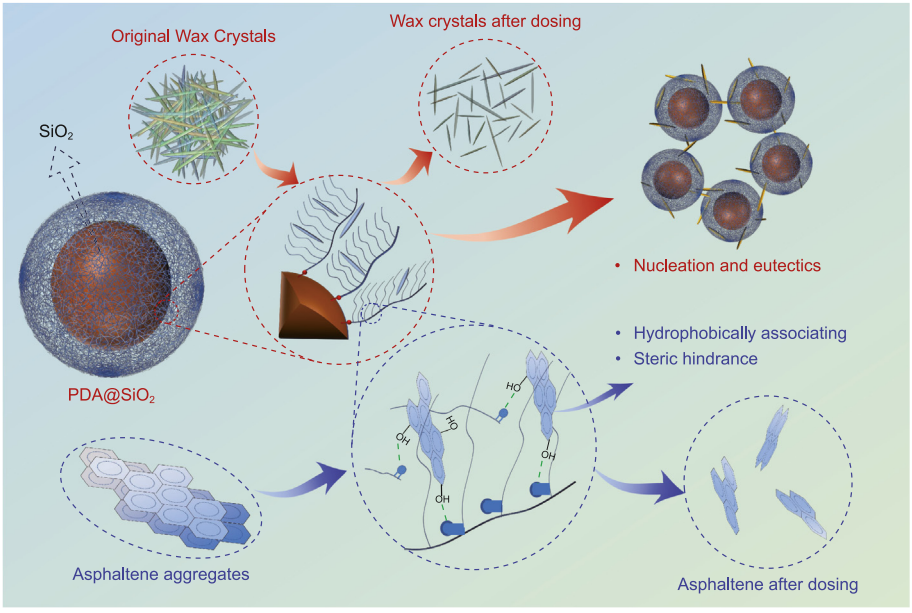

Fig. 13. Possible mechanism of core-shell hybrid nanoparticles inhibiting crystallization of waxes and agglomeration of asphaltenes in crude oil.

4. Conclusion

A series of core-shell nanoparticles by grafting polyacrylate onto the surface of nano-sized SiO_2 were synthesized by solution polymerization method. The study on the wax crystallization behaviors of crude oil show that after adding four types of nano-composite particles, there is no significant change in the WAT of crude oil, but the crystallization enthalpy and wax precipitation amount decrease to varying degrees. In addition, the rheological results indicate that the nanoparticles can not only effectively improving the flowability at low temperature of crude oil, but also obviously decrease the thixotropic area and yield stress. Especially, in the presence of PDA@SiO_2, the wax precipitation amount of crude oil is reduced from 21.05 to 14.74 wt%, the viscosity reduction is 85.6% at 20 °C, the yield stress decreases from 240 to 90 Pa, and the average wax crystal size is reduced by 89.9%. Besides, the agglomeration of asphaltene of crude oil is apparently inhibited, since the IPP is increased from 23% to 29%. Consequently, the improvement of flowability for crude oil is due to the balance of attraction from hydrophobic association and repulsion from steric hindrance provided by the aliphatic branches on the nanoparticles. In summary, the surface grafted polymer nanoparticles exhibit excellent comprehensive properties, which can not only hinder the crystallization growth of wax but also inhibit the settling of asphaltene, which would bring broad application prospects in the fields for crude oil production and pipeline transportation.

CRediT authorship contribution statement

Xin-Yuan Li: Formal analysis, Conceptualization. **Xu-Biao Zhang:** Writing – original draft, Validation, Data curation. **Si-Bei Li:** Methodology, Investigation. **Li-Wei Hui:** Resources. **Xin-Jie Sun:** Visualization, Validation, Software. **Jun Xu:** Writing – review & editing, Project administration, Methodology.

Declaration of competing interest

The authors declare that there are no conflicts of interest, we do not have any possible conflicts of interest.

Acknowledgments

Financial support by project of China Petroleum Engineering Corp., Ltd (CPEC), Study on microstructural regulation of polyacrylate and applying as pour-point depressant for crude oil (2021ZYGC-01-01), is gratefully acknowledged.

Appendix A. Supplementary data

Supplementary data to this article can be found online at https://doi.org/10.1016/j.petsci.2024.06.003.

References

Adeyanju, O.A., Oyekunle, L.O., 2019. Experimental study of water-in-oil emulsion flow on wax deposition in subsea pipelines. J. Petrol. Sci. Eng. 182, 106294. https://doi.org/10.1016/j.petrol.2019.106294.

Alimohammadi, S., Zendehboudi, S., James, L., 2019. A comprehensive review of asphaltene deposition in petroleum reservoirs: Theory, challenges, and tips. Fuel 252 (15), 753–791. https://doi.org/10.1016/j.fuel.2019.03.016.

Belal, J., Maen, M., 2012. Adsorption of asphaltenes from heavy oil onto in situ prepared NiO nanoparticles. J. Colloid Interface Sci. 378 (1), 64–69. https://doi.org/10.1016/j.jcis.2012.04.016.

Corredor, L.M., Husein, M.M., Maini, B.B., 2019. A review of polymer nanohybrids for oil recovery. Adv. Colloid Interface Sci. 272, 102018. https://doi.org/10.1016/j.cis.2019.102018.

Deshmukh, S., Bharambe, D.P., 2008. Synthesis of polymeric pour point depressants for Nada crude oil (Gujarat, India) and its impact on oil rheology. Fuel Process. Technol. 89 (3), 227–233. https://doi.org/10.1016/j.fuproc.2007.10.010.

Gaihre, B., Uswatta, S., Jayasuriya, A.C., 2018. Nano-scale characterization of nano-hydroxyapatite incorporated chitosan particles for bone repair. Colloids Surf. B Biointerfaces 165 (1), 158–164. https://doi.org/10.1016/j.colsurfb.2018.02.034.

Hasan, S.W., Ghannam, M.T., Esmail, N., 2010. Heavy crude oil viscosity reduction and rheology for pipeline transportation. Fuel 89 (5), 1095–1100. https://doi.org/10.1016/j.fuel.2009.12.021.

Huang, H., Wang, W., Peng, Z., et al., 2018. The influence of nanocomposite pour point depressant on the crystallization of waxy oil. Fuel 221 (1), 257–268. https://doi.org/10.1016/j.fuel.2018.01.040.

Jia, H., Hou, W., Wei, L., et al., 2008. The structures and antibacterial properties of nano-SiO_2 supported silver/zinc–silver materials. Dent. Mater. 24 (2), 244–249. https://doi.org/10.1016/j.dental.2007.04.015.

Jing, G., Sun, Z., Tu, Z., et al., 2017. Influence of different vinyl acetate contents on the properties of the copolymer of ethylene and vinyl acetate/modified nano-SiO_2 composite pour-point depressant. Energy Fuel. 31 (6), 5854–5859. https://doi.org/10.1021/acs.energyfuels.7b00189.

Kazemzadeh, Y., Eshraghi, S.E., Kazemi, K., et al., 2015. Behavior of asphaltene adsorption onto the metal oxide nanoparticle surface and its effect on heavy oil recovery. Ind. Eng. Chem. Res. 54 (1), 233–239. https://doi.org/10.1021/ie503797g.

Kumar, R., Dao, E., Mohanty, K.K., 2012. Heavy-oil recovery by in-situ emulsion formation. SPE J. 17 (2), 326–334. https://doi.org/10.2118/129914-PA.

Li, X., Lu, S., Niu, M., et al., 2021. Asphaltene inhibition and flow improvement of crude oil with a high content of asphaltene and wax by polymers bearing ultra-Long side chain. Energies 14 (24), 8243. https://doi.org/10.3390/en14248243.

Li, F., Wang, X., Pan, H., et al., 2019. Preparation of disk-like α-Fe_2O_3 nanocomposites and their catalytic effect on extra heavy crude oil upgrading. Fuel 251 (1), 644–650. https://doi.org/10.1016/j.fuel.2019.04.048.

Li, N., Mao, G., Liu, Y., 2018. Effect of the evaluation and mechanism analysis of a novel nanohybrid pour point depressant on facilitating flow properties of crude oil. Energy Fuels 32 (10), 10563–10570. https://doi.org/10.1021/acs.energyfuels.8b02371.

Liu, Y., Sun, Z., Jing, G., 2021. Synthesis of chemical grafting pour point depressant EVAL-GO and its effect on the rheological properties of Daqing crude oil. Fuel Process. Technol. 223 (1), 107000. https://doi.org/10.1016/j.fuproc.2021.107000.

Mahmoud, T., Betiha, M., 2021. Poly(octadecyl acrylate-co-vinyl neodecanoate)/oleic acid-modified nano-graphene oxide as a pour point depressant and an enhancer of waxy oil transportation. Energy Fuel. 35 (7), 6101–6112. https://doi.org/10.1021/acs.energyfuels.1c00034.

Mao, J., Kang, Z., Yang, X., et al., 2020. Synthesis and performance evaluation of a nanocomposite pour-point depressant and viscosity reducer for high-pour-point heavy oil. Energy Fuel. 34 (7), 7965–7973. https://doi.org/10.1021/acs.energyfuels.9b04487.

Mohammadi, M., Akbari, M., Fakhroueian, Z., 2011. Inhibition of asphaltene precipitation by TiO_2, SiO_2, and ZrO_2 nanofluids. Energy Fuel. 25 (7), 3150–3156. https://doi.org/10.1021/ef2001635.

Ning, X., Song, X., Zhang, S., et al., 2022. Insights into flow improving for waxy crude oil doped with EVA/SiO_2 nanohybrids. ACS Omega 7 (7), 5853–5863. https://doi.org/10.1021/acsomega.1c05953.

Norrman, J., Solberg, A., Sjoblom, J., et al., 2016. Nanocomposites for waxy crudes: effect of polymer coverage and the effect on wax crystallization. Energy Fuel. 30 (6), 5108–5114. https://doi.org/10.1021/acs.energyfuels.6b00286.

Oyekunle, L., Adeyanju, O., 2011. Thermodynamic prediction of paraffin wax precipitation in crude oil pipelines. Petrol. Sci. Technol. 29 (2), 208–217. https://doi.org/10.1080/10916460903330163.

Qing, Y., Yang, M., Li, L., et al., 2020. Effect of organically modified nano silica on the viscosity and rheological behavior of karamay heavy crude oil. Energy Fuel. 34 (1), 65–73. https://doi.org/10.1021/acs.energyfuels.9b01325.

Soni, H.P., Bharambe, D.P., 2008. Performance-based designing of wax crystal growth inhibitors. Energy Fuel. 22 (6), 3930–3938. https://doi.org/10.1021/ef8002763.

Soni, H.P., Agrawal, K.S., Nagar, A., et al., 2010. Designing maleic anhydride-α-olifin copolymeric combs as wax crystal growth nucleators. Fuel Process. Technol. 91 (9), 997–1004. https://doi.org/10.1016/j.fuproc.2010.02.019.

Taborda, E.A., Alvarado, V., Cortés, F.B., 2017. Effect of SiO_2-based nano fluids in the reduction of naphtha consumption for heavy and extra-heavy oils transport: economic impacts on the Colombian market. Energy Convers. Manag. 148 (15), 30–42. https://doi.org/10.1016/j.enconman.2017.05.055.

Yan, Y., Cui, Y., Jiang, W., et al., 2017. Drag reduction in reservoir rock surface: hydrophobic modification by SiO_2 nanofluids. Appl. Surf. Sci. 396 (28), 1556–1561. https://doi.org/10.1016/j.apsusc.2016.11.209.

Yang, F., Paso, K., Norrman, J., et al., 2015. Hydrophilic nanocomposites facilitate wax inhibition. Energy Fuel. 29 (3), 1368–1374. https://doi.org/10.1021/ef502392g.

Yao, B., Li, C., Yang, F., et al., 2016a. Organically modified nano-clay facilitates pour point depressing activity of polyoctadecylacrylate. Fuel 166 (15), 96–105. https://doi.org/10.1016/j.fuel.2015.10.114.

Yao, B., Li, C., Yang, F., et al., 2016b. Structural properties of gelled Changqing waxy crude oil benefitted with nanocomposite pour point depressant. Fuel 184 (15), 544–554. https://doi.org/10.1016/j.fuel.2016.07.056.